計測自動制御学会東北支部 第 161 回研究集会 (1996.6.28)
資料番号 161-4

Monitoring and Classification of Coolant State in Nuclear Reactor

G. ロストン, R. コスマ, 北村 正晴

Graciela Roston, Robert Kozma, Masaharu Kitamura

東北大学

Tohoku University

キーワード： cross-correlation technique, transit time, frequency dependent analysis, void fraction fluctuation, variance of void fraction

連絡先： 〒980-77 Quantum Science and Energy Engineering Department. Tohoku University. Aramaki-Aza, Aoba, Sendai , Japan

Tel.: (022)217-7907, Fax.: (022)217-7907, E-mail: graciela@minei.nucle.tohoku.ac.jp

1. Introduction

An important feature of Boiling Water Reactor (BWR) is a detailed description of the coolant flow condition in individual fuel bundles. When the coolant is a two-phase mixture of liquid and vapor, the coolant flow pattern can become quite complicated. In vertical two-phase flows, the following basic flow regimes can be defined: bubbly, slug, churn and annular.

A transit time can be associated with the axial propagation of the coolant density fluctuations. The measurement technique for transit time by means of cross-correlation of the signals (randomly time varying boiling noise pattern) of two axially displaced detectors has been applied [1) 2)]. Both detectors are affected by the travelling disturbance, but the down stream signal is shifted with a time delay which is equal to the time for the disturbance to travel from the upstream detector to the down stream detector. A peak occurs in the cross-correlation function at the transit time τ of the travelling disturbance. This is due to the definition:

$$\frac{1}{T}\int_{-T2}^{T2} x(t)y(t+\tau)dt = R_{xy} \qquad (1)$$

The determination of the delay time between the two signals may also be performed in the frequency domain. The mathematically equivalent function is then the Cross Power Spectral Density (CPSD). The transit time in this case is given by the linear slope of the phase of this complex function:

$$[magnitude(f)] * \exp(-i2\pi f\tau) = CPSD(f) \qquad (2)$$

and

$$\frac{1}{2\pi} * \frac{d\theta}{dt} = \tau \qquad (3)$$

where θ is the phase angle. The coherence function $\gamma^2(f)$ of two quantities $x(t)$ and $y(t)$ is defined as:

$$\frac{\|CPSD_{xy}(f)\|^2}{APSD_x(f) * APSD_y(f)} = \gamma^2 \qquad (4)$$

As this ordinary coherence function measures the extent to which $y(t)$ may be predicted from $x(t)$, in order to obtain an estimate of how the signal pattern changes between the two detectors, the coherence function was used.

The Local Power Range Monitors (LPRM) data have been represented by the corresponding probability density function (pdf). This function is the relative density with which the value x appears in the collection of data, and is an estimate of the rate of change of probability with magnitude [2].

The square of the root mean square RMS^2, which is the variance of the signal fluctuation, was calculated over an entire band between f_1 and f_2 as follows:

$$\int_{f_1}^{f_2} APSD(f)df = RMS^2 \qquad (5)$$

It should be noted here that estimation of time delay by means of cross correlation analysis is an established technique, if the quality of the observed signals is reasonably good. In our analysis with signals measured at a BWR, the measured variable is neutron fluctuation since we can not install ordinary flow monitors (optical, impedance, etc) within the reactor because of experimental limitations. The neutronic signal can be disturbed not only by bubbles in the coolant flow but also by other quantities, e.g. temperature nonuniformity, flow regime, flow distribution within the coolant channel, etc. Detailed treatment of the fluctuations is needed in this regard.

2. Methodology

The data were taken from a 900MW BWR Nuclear Power Plant, the measurement conditions were: reactor power: 64%, core flow: 4220Kg/sec, Fs=5Hz. LPRM D, LPRM C, LPRM B and LPRM A are in the same string; where LPRM D is in the the top of the core.

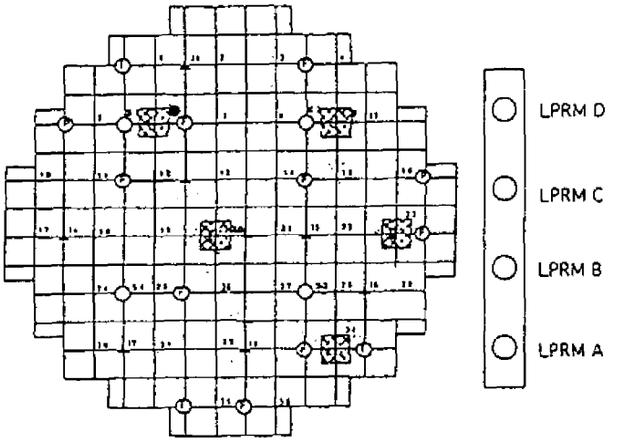

Fig. 1 Reactor core and detector string

In general, an in-core detector will see the sum of local and global effects. With this in mind, we introduced a simple preprocessing of the signal. From each detector signal we subtracted the average of the four detectors in one string to remove global noise component (from now on case (b)).

For a given frequency range the coherence values were taken from:

$$\frac{1}{f_1 - f_2} * \int_{f_1}^{f_2} \gamma^2 df = \bar{\gamma}^2 \qquad (6)$$

The phase angle was calculated in a frequency range corresponding to coherence values greater than 0.4.

For the calculation of the pdf of each signal we took the half data points at the beginning and at

the last, for a better comparison. Bubbly and annular flows have unimodal character, e.g. their pdf is single peaked. Slugs flows are classified as bimodal and they have pdf with two peaks. The modality of the flows is related to the moments of the pdf. This relation has been investigated [3] in order to develop an objective flow regime indicator. The assumption concerning spatial and temporal independence of bubbles is definitely not valid in slug flows, due to the presence of a well-defined spatial and temporal correlation in the void fraction fluctuation signal. Part of the difficulties can be solved by introducing a modified binomial model in which certain time-correlations are incorporated. The modified model is based on the bimodal approximation of void fraction fluctuations in two-phase flows [4].

We used this model in order to see changes of the intensity of the void fractions fluctuations along the channel. The bimodal two-phase flow model is determined by the following set of parameters: μ_1, μ_2, σ_1^2 and σ_2^2 which are the expected values and variance of the first and second mode respectively. The variance of the bimodal mixture is the sum of weighted variances of the separate modes and an additional term, which depends on the difference between the expected values of the two modes and on their relative frequency of occurrence. In order to develop an objective indicator, eliminating the characteristic constant and the background of each detector, we calculate:

$$\frac{(\mu_1 - \mu_2)^2}{\sigma_1^2 - \sigma_2^2} = z \qquad (7)$$

3. Observations

In Fig.2 the Coherence and Phase between two LPRM are given for case (a), without subtraction, in the left side, and case (b) in the right side. When applying case (b) we get a better linearity in the phase, mainly at frequencies higher than 1Hz. Also the frequency band of coherence values higher than 0.4 is larger. As while approoaching to the bottom of the core, the phase is not linear(it has some interesting fluctuations) and the coherence values are lower than o.4Hz.

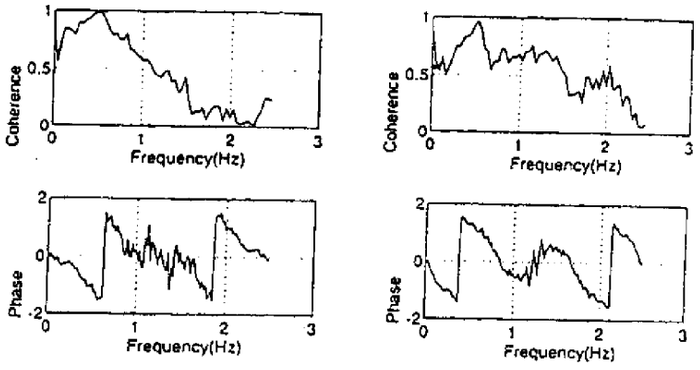

Fig. 2 LPRM C and LPRM D

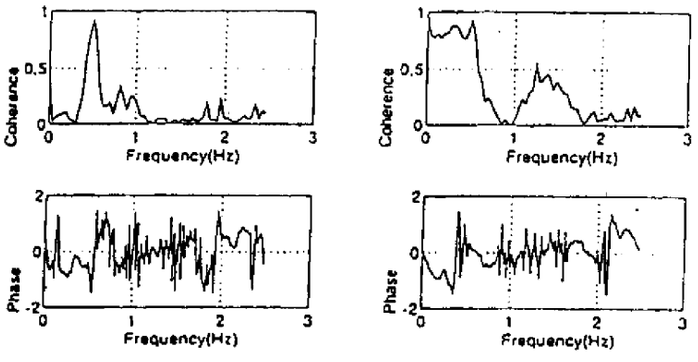

Fig. 3 LPRM A and LPRM D

The phase between LPRM B and LPRM D shows two different and well defined slopes. For both cases, and between all the LPRM, the calculation and analysis clearly show that a core resonance phenomenon leads to oscillations at 0.5Hz which are representative of the well-known BWR stabil-

ity problem [5].

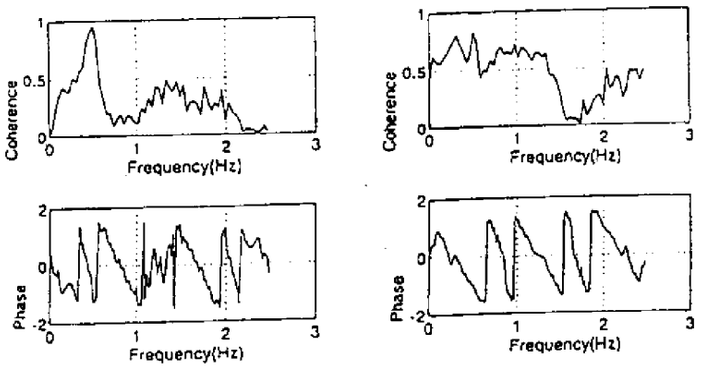

Fig. 4 LPRM B annd LPRM D

Table I shows the obtained time delay for different frequency bands, taking in account the coherence values. From this table, we can see that the correspondent results for both cases significantly differed for frequencies higher than 1Hz.

LPRM D and LPRM C					
Freq. Band (Hz)		Coherence		T (sec)	
Case(a)	Case(b)	Case(a)	Case(b)	Case(a)	Case(b)
0 : 0.63	0 : 0.35	0.867	0.683	0.37	0.31
0.63 : 1.1	0.35 : 1.2	0.695	0.729	0.51	0.44
1.1 : 1.4	1.2 : 2.1	0.430	0.495	0.65	0.36

Table 1 Time Delay for LPRM D and C

Fig. 5 summarizes the calculation on the four detectors using the phase angle and the cross correlation. In the first method, we took the mean weighted by both the frequency band and the coherence values along all the frequencies to compare these values with those obtained from the latter one. Only in case (b), we could calculate the time delay using the displacement of the Cross Correlation peak. In the figure, crosses and circles means results obtained applying the phase shift calculation for case (a), without subtraction, and case (b), with a preprocessing of the signal respectively. Results obtained using the displacement of the cross correlation are marked with an asterisk.

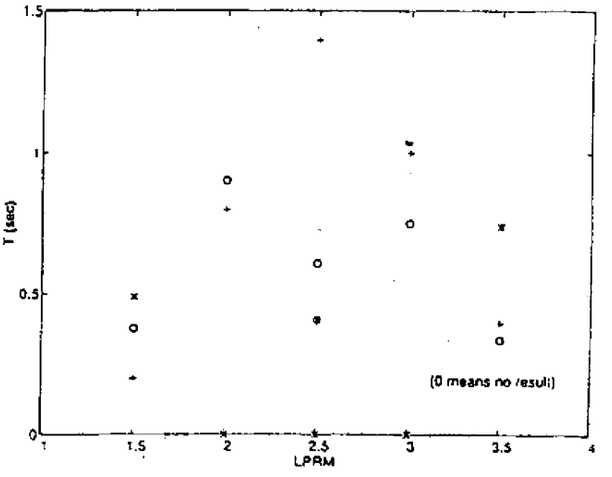

Fig. 5 Time Delay Calculation

Time delay along the channel (sec)			
Signal	0.1: 0.4(Hz)	0.6 : 1 (Hz)	0 : 2 (Hz)
LPRM DC	0.314	0.435	0.376
LPRM CB	0.404	0.404	0.417
LPRM DB	0.759	1.410	0.900

Table 2 Time delay along the channel

The results obtained applying the displacement of the cross correlation peak do not fulfill the additivity of the transit time. Additivity means:

$$T_{12} + T_{23} = T_{13}$$

where T_{12} is the transit time measured between detectors 1 and 2 in the same string. The best approximation for the additivity of the transit time is

observed at frequencies higher than 1 Hz or below 0.4 Hz.

The RMS^2 has been determined over various frequency regions according to (5). The results, which are showed in Table 3, significantly vary for different frequency regions. At low frecuencies there is an increasing of the RMS^2 while at high frecuency range a decreasing is observed.

RMS2				
F (Hz)	LPRM D	LPRM C	LPRM B	LPRM A
0 : 0.19	2.894	2.961	8.703	18.967
0.19 : 0.78	102.865	103.093	97.497	88.591
0.78 : 2.46	7.729	7.385	7.274	5.340
0 : 2.46	113.488	113.439	113.474	112.898

Table 3 RMS^2 over various frequency regions

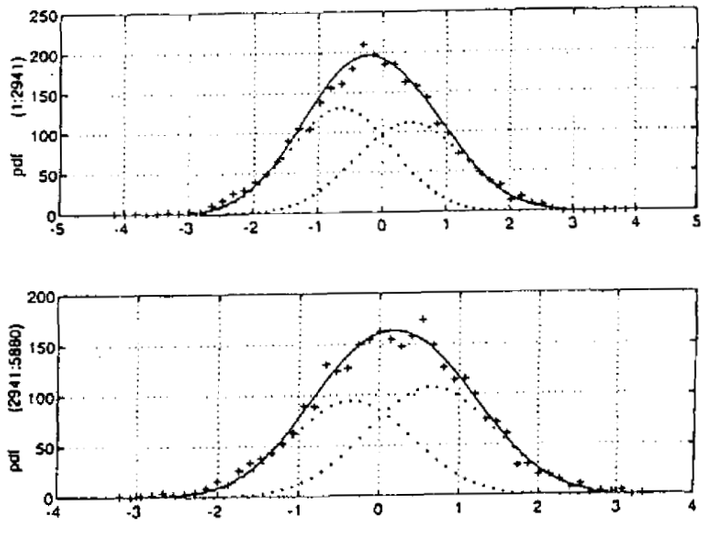

Fig. 6 Results of the binormal fit of the pdf for LPRM D

In Fig.6, result of binormal fit of the pdf of LPRM D is shown. Crosses denote points of the calculated pdf having 50 channels; solid line shows the binormal fit and punctuated lines indicate the two Gaussian componentof the fit.

Similar fit has been performed for the other 3 LPRM and the results are summarized in Table 4. Here, the expected values and the variances in each mode change for different signals, and also between the first and last data points.

Gaussian fitting										
	From pdf(1:2940)					From pdf (2941:5580				
LPRM	μ_1	μ_2	σ_1	σ_2	z	μ_1	μ_2	σ_1	σ_2	z
D	0.4	-0.6	0.8	0.8	17	0.7	-0.3	0.8	0.8	16
C	0.3	-0.5	0.8	0.8	11	0.6	-0.4	0.8	0.8	12
B	0.6	-0.5	0.9	0.7	8	0.5	-0.4	0.9	0.7	7
A	0.6	-0.3	1	0.8	2	0.3	-0.5	0.9	0.7	3

Table 4 Gaussian fitting of the four LPRM

4. Discussion

Due to the removal of the low frequency global noise, the frequency band of high coherence values greater than 0.4 increases. This effect also permits a better resolution in the linearity of the phase. Between LPRM D and LPRM A, for this vertical spacing the hydraulic turbulence and additional void generation practically wipe out bubble patterns over this distance. The mechanism responsible for the interesting fluctuations in the phase while approaching to the bottom of the core can not be explained at this point. Possibly due to the fact that LPRM signals oscillate in phase throught the whole core and the strongest oscillation is found in the environment of 9x9 fuel (correspondent to the measured string) [5], the phase between LPRM D and LPRM B shows two different slopes.

The decreasing of the RMS^2 at high frequencies (from the top to the bottom) can be understood on the basis of the bimodal two-phase flow model, where the RMS^2 at high frequencies is proportional to the void fraction [6].

In the framework of the study, at this point, it is difficult to find a reason to explain the changes of the expected values and the variances obtained from the bimodal fit for different signals and also between the first and last data point.

5. Conclusions

The results obtained applying the displacement of the cross correlation peak do not fulfill the additivity of the transit time. The best approximation for this additivity was obtained applying the coherence based frequency analysis of the phase shift of the CPSD.

When the measured variable is neutron fluctuation, is better to calculate the transit time for different frequencies, according to high coherence values, in order to get more realible results .

In our calculation, when the signal was preprocessed by removing the global noise component, the results were improved.

参考文献

1) Thie J.: Power Reactor Noise, 159/163 American Nuclear Society (1981).
2) Bendat J., Piersol A.: Random Data Analysis and Measurements Procedures,48/50 John Wiley and Sons (1986).
3) Vince M. and Lahey R. : On the development of an objective flow regime indicator. Int. J. Multiphase Flow 8, 93/124 (1984).
4) Kozma R.: Studies on the relationship between the statistics ofvoid fraction fluctuations and the parameters of two-phase flows. Int. J. Multiphase Flow 21, 241/251 (1995).
5) Bergdahl B., Reisch F. , Oguma R.: BWR stability investigation at ForsmarkI. Ann. Nucl. Energy Vol 16-10, 509/520 (1989).
6) Kozma R., Kitamura M.,Hoogenboom : Void fraction measurement in nuclear reactors via neutron noise methods. Paper submited for publication to Nuclear Technology (1995).